frontiers | Frontiers in Energy Research

ORIGINAL RESEARCH
published: 01 July 2022
doi: 10.3389/fenrg.2022.931890

Optimal Dispatching Modeling of Regional Power–Heat–Gas Interconnection Based on Multi-Type Load Adjustability

Bowen Wang[1], *Hongbin Sun*[2] *and Xiaosong Song*[3]*

[1]School of Electrical Engineering, Northeast Electric Power University, Jilin, China, [2]School of Computer Technology and Engineering, Changchun Institute of Technology, Changchun, China, [3]State Grid Changchun Power Supply Company Substation Operation and Maintenance Center, Changchun, China

As an important research direction of the energy system, the integrated energy system of a park plays an important role in the field of energy optimization and sustainable economic operation. In this study, a low-carbon optimal operation model of the integrated energy system of an industrial park is proposed, considering a controllable flexible load response. First, the typical structure of the integrated energy system of the park and the model of each subsystem are introduced; then, under the premise that flexible electrical and thermal loads can be used for adjustment of energy utilization, a complete dispatch scheme is constructed according to the energy consumption and system operation characteristics of the integrated energy system. Finally, an optimal scheduling model for the combined supply and demand of the integrated energy system is established with the aim of minimizing the total operating cost. For experimental results, the YALMIP toolbox and the CPLEX solver are used to verify the results of the study; simulation results show that the optimal scheduling of controllable loads can effectively reduce the comprehensive operating cost of a community integrated energy system.

Keywords: integrated energy system, flexible load, carbon trading, optimal dispatch, load adjustability

OPEN ACCESS

Edited by:
Chen Chen,
Xi'an Jiaotong University, China

Reviewed by:
Jian Wang,
Southwest Jiaotong University, China
Bao Liu,
China Universtiy of Petroleom, China
Li Wanggen,
AHNU, China

***Correspondence:**
Xiaosong Song
2509860227@qq.com

Specialty section:
This article was submitted to Smart Grids, a section of the journal Frontiers in Energy Research

Received: *29 April 2022*
Accepted: *26 May 2022*
Published: *01 July 2022*

Citation:
Wang B, Sun H and Song X (2022) Optimal Dispatching Modeling of Regional Power–Heat–Gas Interconnection Based on Multi-Type Load Adjustability. Front. Energy Res. 10:931890. doi: 10.3389/fenrg.2022.931890

INTRODUCTION

Considering the diversity and scale of energy demand in industrial parks, industrial energy conservation has become a main theme of energy conservation. The community integrated energy system (IES) has controllable new energy units; gas units; energy storage devices; and cold, heat, and electricity loads, constituting a variety of heterogeneous energy complementing energy supply and demand systems, which can not only improve energy utilization efficiency but also meet various load needs. Therefore, industrial parks have become the main application object of IES. IES couples electricity, heat, and gas systems to coordinate the conversion of multiple energy sources within an industrial park. At present, research on IES scheduling methods has mainly focused on equipment modeling and energy supply structure. To address the scheduling problem of electric integrated energy systems, Katiraei et al. (2008) proposed an energy hub (EH) model type, which has been widely used in research related to an intermediate for integrated energy systems such as optimizing scheduling and energy consumption. With the continuous development of energy utilization technology, load side management has also received more and more attention, and flexible load scheduling plays an important role in energy consumption. The load in the microgrid

can be roughly divided into three categories according to scheduling capacity, namely, important load, adjustable load, and translational load (Hatziargyriou et al., 2007; Stluka et al., 2011). Basic loads must be powered within a specific period of time, such as lighting; adjustable loads refer to loads where users cannot use electricity according to plan and demand variable loads, such as air conditioning and heating; shiftable loads refer to loads whose load power supply time can be changed according to plans, such as washing machines and disinfection cabinets (Alipour et al., 2018). Dolatabadi and Mohammadi-Ivatloo (2017) established an optimal operating model of a multi-energy system consisting of a multi-energy carrier production and transmission system and a connected smart EH, with the aim of minimizing energy supply costs and maximizing user satisfaction, adjusting the energy consumption of end users according to the energy prices published by the system operator and formulating internal operating plans. Chen et al. (2015) established an optimization model of various energy supply modes including cogeneration, wind energy, via an electric boiler, and heat storage, and the introduction of electric boilers and heat storage devices was verified to improve the flexibility of cogeneration and effectively reduce the role of curtailed wind power. Li et al. (2016) indicated that the use of heat storage capacity of the district heating network to coordinate the short-term operation of the power and district heating system effectively promoted the wind power grid and optimal operation of the system. In addition, due to the deepening of the connection between electric load equipment, the heat load response presents peak shaving and valley filling values, as confirmed by the application of user-side load response in the power system. Therefore, it is imperative to explore the dispatchable value of demand-side electricity and heat loads in park IES, and study the collaborative control and scheduling optimization of multiple-load response capabilities on the user-side of the IES, to achieve optimal utilization of various load resources.

The major contributions of this study are as follows: this study establishes a park integrated energy system including wind turbine (WT), photovoltaics (PV), natural gas micro-combustion engine (micro-gas turbine, MT), gas turbine (GT), gas boiler (GB), bromine cooler (lithium bromide refrigerator, LBR), energy storage systems, and loads. Based on existing research, with the dispatchable value of multiple loads in the comprehensive energy system management, an economic operation dispatch model considering the demand response is proposed, and the transmission characteristics of the heat load and the electric load are studied, which shows that the dispatch model considering the electric load response plays an important role in energy consumption in the proposed demand response.

When the controllable load of cold and heat participates in the dispatch of the integrated energy system, considering the economic optimization of the previous dispatch, a target function considering the flexible dispatch of load under the carbon trading mechanism is proposed. In this model, the consumption of new energy is also maximized. The CPLEX solution objective function in the Yamalab toolbox was called. CPLEX is very powerful IBM-developed optimization software, which can also support parallel computing, C, C++, Java, MATLAB, and other software interface programming and can also be used directly with the own IDE for programming; the performance of the official programming language for OPL is better. By comparing the two scenarios, you can intuitively derive the superiority of the model proposed in the article.

The remainder of this article is organized as follows. The second part discusses the equipment model within the park's integrated energy system. The third part discusses load models, including transferable loads, interruptible loads, and translatable loads, as well as their constraints. The fourth part discusses the objective function of the economic operation of the park and the constraints of the park system. Conclusion and analysis are presented in the last part.

INTEGRATED ENERGY SYSTEM ARCHITECTURE OF THE PARK

The IES structure and energy flow of the park studied in this article are shown in **Figure 1**, including energy conversion equipment, energy supply side, and three parts of the electric–thermal load demand response. The park's integrated energy system consists of WT, PV, natural gas micro-combustion engine (MT), GT, GB, bromine cooler (LBR), electrical energy storage (ES), heat storage (HS), cold storage (CS), electrical load, cooling load, and heat load. The electric load of the park comprises WT, PV units, and natural gas internal combustion engines, with excess electricity being stored in batteries, while the thermal load is supplied by the waste heat of the MT, electric heating equipment, GB, and the excess heat is stored.

Fuel Cell

A fuel cell (FC) is a chemical device that directly converts the chemical energy of fuel into electrical energy without other media, and directly converts the chemical energy of fuel and oxidant into electrical energy through electrochemical reactions. The FC can theoretically operate at a thermal efficiency close to 100%, which is highly economical. This study considers that the FC is mainly responsible for electrical energy dispatching in the day-ahead dispatching, and its thermal energy is no longer considered here. The electrical power output of the fuel cell can be expressed as,

$$P_{\min}^{FC} \le P^{FC} \le (1-\omega_{FC})P_{\max}^{FC}, \tag{1}$$

where

P^{FC} indicates the output power of the FC, kW;
$P_{\min}^{FC}$ indicates the minimum output power of the FC, kW;
$P_{\max}^{FC}$ indicates the maximum output power of the FC, kW; and
ω_{FC} represents the standby coefficient of the FC, at 0.45.

The amount of natural gas consumed by FCs, G_{FC} can be expressed as:

$$G_{FC} = \frac{P^{FC}}{\eta_{FC} L_{NG}}, \tag{2}$$

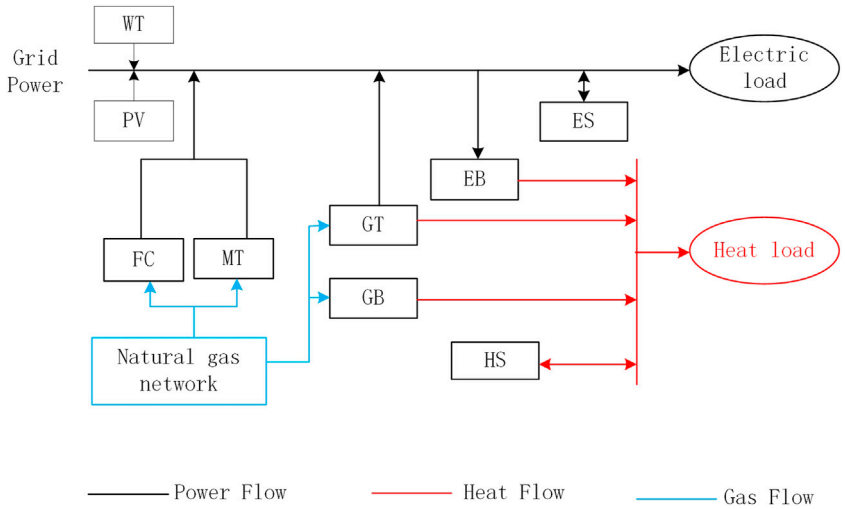

FIGURE 1 | IES structure and energy flow.

where η_{FC} represents the power generation efficiency of the FC, at 0.85; L_{NG} represents the low calorific value of natural gas, at 9.8 kWh/m^3.

Storage Battery

A storage battery is a device that directly converts chemical energy into electrical energy. It is a rechargeable battery designed to be recharged through a reversible chemical reaction. To protect the battery life from being affected by overcharging and discharging, we must constrain the output and state of charge (SOC) of the battery.

$$\text{Battery output restriction}: P_{\min}^{BAT} \le P^{BAT} \le P_{\max}^{BAT}, \tag{3}$$

where P^{BAT} indicates the output state of the battery, $P^{BAT} > 0$ indicates electricity storage, and $P^{BAT} < 0$ indicates discharge, kW;

$P_{\min}^{BAT}$ indicates the minimum discharge power of the battery, kW; and

$P_{\max}^{BAT}$ indicates the maximum storage power of the battery, kW。.

$$\text{Battery SOC constraints}: \begin{cases} S_{\min} \le S_{SOC} \le S_{\max} \\ S_k = S_t \end{cases}, \tag{4}$$

where

S_{SOC} indicates the charged state of the battery,

$S_{\min}$ indicates the minimum battery SOC,

$S_{\max}$ indicates the maximum battery SOC,

S_k indicates the SOC when the battery starts to charge, and

S_t indicates the SOC at the end of battery charging.

Energy Storage Equipment

The two energy storage devices, HS tank and CS tank, can be represented by a unified energy storage model, in terms of energy conversion. The energy storage equipment will be constrained by the upper and lower limits of the energy storage capacity and charging and discharging power when the system is running. The specific mathematical model (Yang et al., 2021a) is as follows:

$$E_t^S = E_{t-1}^s (1 - \eta_{loss}) + \eta_{char} P_{char,t}^S \Delta t - \frac{P_{dis,t}^S}{\eta_{dis}}, \tag{5}$$

where E_t^S indicates the storage capacity of the energy storage device in the t period;

$P_{char,t}^S$ represents the charging power of the energy storage device during the period t;

$P_{dis,t}^S$ represents the discharge power of the energy storage device in the period t; and

η_{loss}, η_{char}, and η_{dis} are the self-loss rate, charging efficiency, and discharging efficiency of the energy storage device, respectively.

$$\text{Restrictions}: \begin{cases} E_{\min} \le E_t^S \le E_{\max} \\ 0 \le P_{char,t}^S \le \alpha_{char,t} P_{char,t} \\ 0 \le P_{dis,t}^S \le \alpha_{dis,t} P_{dis,t} \\ \alpha_{dis,t} + \alpha_{char,t} \le 1 \\ E_1 = E_T \end{cases}, \tag{6}$$

where $E_{\max}$ and $E_{\min}$ indicate the upper and lower limits of the energy storage capacity of the energy storage device, respectively. $\alpha_{dis,t}$ and $\alpha_{char,t}$ indicate the discharge and charging state of the energy storage device, which is a variable of 0 and 1, respectively; 1 indicates that the energy storage device is in the charging or discharging state, while 0 indicates that the energy storage device is stationary, that is, charging and discharging is stopped.

Lithium Bromide Refrigerator

The heat of the heating grid is used to heat the lithium bromide water solution to drive the refrigerator to work. The cooling capacity per unit time can be expressed as:

$$R_t^a = Q_t^i C_{OP}, \tag{7}$$

where

C_{OP} represents the cooling coefficient of LBR at 1.20,
R_t^a indicates the cooling capacity in the period t, and
Q_t^i indicates the heat of the heating source in the period t.

Gas Boilers and Micro-Gas Turbines

The relationship between the heat supply of the GB (Vasilj et al., 2019) and the rated heat supply (Li et al., 2015) is given by:

$$Q_{GB} = R_{GB}\eta_{GB}, \tag{8}$$

where

Q_{GB} indicates the output heat value of the boiler,
R_{GB} indicates the rated heat supply of the boiler, and
η_{GB} represents the thermal efficiency of the boiler at 0.9.

The relationship between the heat generated by the MT and the output electric power (Yang et al., 2021b) is given by:

$$Q_t^{MT} = \frac{P_t^{MT}\left(1 - \eta_e - \eta_{loss}\right)}{\eta_{loss}}, \tag{9}$$

where

Q_t^{MT} represents the MT exhaust waste heat in period t,
P_t^{MT} represents the output electric power of MT in period t,
η_e is the efficiency of the MT at 0.2, and
η_{loss} represents the heat loss of MT at 2%.

The amount of natural gas consumed by MT can be expressed (Yang et al., 2021b) as:

$$V_t^{MT} = \frac{P_t^e \Delta t}{\eta_e L_{NG}}, \tag{10}$$

where V_t^{MT} indicates the amount of natural gas consumed by MT in period t and

L_{NG} represents the low calorific value of natural gas, at 9.8 kWh/m^3. Δt indicates that the time step is 1 h.

Climbing constraints for MT units are expressed as:

$$P_{down}^{MT} \le P_t^{MT} - P_{t-1}^{MT} \le P_{up}^{MT}, \tag{11}$$

where P_{down}^{MT} and P_{up}^{MT} indicate the maximum descending and ascending rates of MT, respectively, which are both considered 85 kW/h in this study.

LOAD MODEL

The controllable load in the comprehensive energy system of the park can be divided into three categories: important load, translational load, and adjustable load according to the energy consumption characteristics. Considering the flexibility of the load, the transfer characteristics of the heating load and the cooling load are not considered here (Chen et al., 2021). Translatable load refers to when the power supply time of the load can flexibly change the load according to the operating state of the IES. The translation of this type of load will not change the total load of the entire scheduling period; hence, it will not affect the total power demand of users.

Expressions for Translatable Loads

The translatable load is more flexible than the shiftable load. For this type of load, the total amount of the transferred load under the condition is unchanged, and the power of each period can be reasonably adjusted according to the charging state characteristics of a private electric vehicle, and its charging power and time can be changed based on the amount of charge it needs.

$$\begin{cases} \min \sum_t^T \left(S_t - S_{obj,t}\right)^2 \\ S_t = S_t^{fore} + S_{in,t} - S_{out,t} \end{cases}, \tag{12}$$

where T represents the scheduling period; S_t is the load value in the period t after the shift; $S_{obj,t}$ is the target load value in period t; S_t^{fore} is the load forecast value for the period t scheduled for the day before; and $S_{in,t}$ and $S_{out,t}$ are the translatable load values transferred in and out in the period t, respectively. Considering that the load transferred in or out before period t may affect the load in period t, the expressions of $S_{in,t}$ and $S_{out,t}$ (Hinton et al., 2019) are:

$$\begin{cases} S_{in,t} = \sum_{\substack{m=1 \\ m \ne t}}^{T} \sum_{k=1}^{K_{total}} u_{k,m,t} S_{l,k} + \sum_{l=1}^{L} \sum_{\substack{m=1 \\ m \ne t-l}}^{T} \sum_{k=1}^{K_{total}} u_{k,m,(t-l)} S_{l+1,k} \\ S_{out,t} = \sum_{\substack{m=1 \\ m \ne t}}^{T} \sum_{k=1}^{K_{total}} u_{k,m,t} S_{l,k} + \sum_{l=1}^{L} \sum_{\substack{m=1 \\ m \ne t-l}}^{T} \sum_{k=1}^{K_{total}} u_{k,m,(t-l)} S_{l+1,k} \end{cases}, \tag{13}$$

where T represents the scheduling period; K_{total} represents the type of load that can be translated; $u_{k,m,t}$ represents the number of shiftable loads of type k transferred from period m to period t; $S_{1,k}$ represents the k-th shiftable load in the first working period load value; l is the maximum working time of the translatable load; and $S_{l+1,k}$ indicates the load value of the k-th shiftable load in the $l + 1$ period.

Restrictions

The constraints are as follows:

$$\begin{cases} u_{k,t} = \sum_{t'=1}^{T} u_{k,t,t'} \\ \forall t, t', k \quad u_{k,t,t'} \ge 0 \\ u_{k,t,t'}, \quad \left|t - t'\right| > d_k \end{cases}, \tag{14}$$

where $u_{k,t}$ indicates the number of loads that can be shifted in the k-th load in the period t, and d_k represents the k-th negative load translation time margin.

Shiftable Load Objective Function of the Integrated Energy System in the Park

The energy-using characteristics of a shiftable load require that it cannot be interrupted during energy use and only allows the load energy consumption period to be panned to another time period

as a whole, such as washing machines, water heaters, and ice machines.

Cooling load objective function:

$$\begin{cases} \min \sum_{t=1}^{T} \left(C_t^{load} - C_t^{obj,load} \right)^2, \\ C_t^{obj,load} = P_t^{load} C_{OF} \end{cases} \tag{15}$$

where C_t^{load} is the shifted cooling load value at time period t; $C_t^{obj,load}$ indicates the target value of cooling load in period t; C_{OP} represents the cooling coefficient of the LBR, at 1.20; and P_t^{load} represents the shifted electrical load value in the period t. Thus, the heat load objective function is:

$$\begin{cases} \min \sum_{t=1}^{T} \left(H_t^{load} - H_t^{obj,load} \right)^2, \\ H_t^{obj,load} = P_t^{load} H_{CE} \end{cases} \tag{16}$$

where H_t^{load} represents the shifted heat load value at time period t; $H_t^{obj,load}$ indicates the target value of the heat load in the period t; and H_{CE} represents the rated thermoelectric ratio of the MT.

The electric load objective function is given by:

$$\begin{cases} \min \sum_{t=1}^{T} \left(P_t^{load} - P_t^{obj,load} \right)^2, \\ P_t^{obj,load} = \dfrac{\dfrac{1}{K(t)}}{\sum_{i=1}^{24} \dfrac{1}{K(i)}} \sum_{i=1}^{24} P_t^{fore,load}, \end{cases} \tag{17}$$

where P_t^{load} represents the shifted electrical load value in the period t; $P_t^{obj,load}$ represents the target value of the electrical load in the period t; $P_t^{fore,load}$ represents the predicted value of the electric load in the period t; $K(t)$ indicates the electricity sales price of the grid in the same time period.

INDUSTRIAL PARK INTEGRATED ENERGY SYSTEM OPTIMAL SCHEDULING MODEL

In this study, a short-term forecast of the translatable electric heating and the cooling load was carried out, and the output of WTs and PV units was considered to ensure the economy and stability of the operation of the park while meeting the various constraints of the comprehensive energy system of the park. In the scheduling plan, the scheduling cost of the shiftable load, the operating cost of the unit, environmental cost (mainly considering the penalty cost of $\rho_a * V_K * c_a * dT_{in}^{on}(t) = Q_t * dt + Q_{new} * dt - Q_{TCLs} * dt$ emission), interaction cost with the external network such as the cost of buying natural gas, and the consumption cost of natural gas for gas equipment were mainly considered. While weighting the minimum value of each cost, the impact of the scheduling of shiftable loads on the scheduling flexibility of the IES in the park and the accommodation of WTs and PV were considered.

The objective function of day-ahead scheduling with a minimum comprehensive running cost in one cycle is given by:

$$\min F = F_1 + F_2 + F_3 + F_4, \tag{18}$$

$$\begin{cases} F_1 = \sum_{t=1}^{T} \left\{ K_{WT} P_{WT}(t) + K_{PV} P_{PV}(t) + C_{gas} \left[V_{MT}(t) + V_{GB}(t) + V_{FC}(t) \right] \right\}, \\ F_2 = \sum_{t=1}^{T} K_{grid} P_{grid}(t), \\ F_3 = F^{trans} + \sum_{n=1}^{3} F_n^{sh} + F_n^{cut}, \\ F_4 = \sum_{t=1}^{T} K_c \left[\eta_1 P_{MT}(t) + \eta_2 P_{GB}(t) + \eta_3 P_{FC}(t) \right], \end{cases} \tag{19}$$

where F_1 represents the operating cost of the units in the IES in the park; K_{WT} represents the operating cost coefficient of WT, in yuan; $P_{WT}(t)$ represents the output power of the WT in the period t, kW; K_{PV} represents the operating cost coefficient of PV units, in yuan; $P_{PV}(t)$ represents the output electric power of the photovoltaic unit in period t, kW; C_{gas} represents the natural gas price, per unit yuan/m^3; $V_{MT}(t)$, $V_{GB}(t)$, and $V_{FC}(t)$ represents the amount of natural gas consumed by MT, GB, and FC in period t, m^3; F_2 represents the electricity purchasing cost of interconnected power grid, yuan; K_{grid} represents the time-of-use electricity price per unit of power, in yuan; $P_{grid}(t)$ refers to the power purchased from the large power grid in period t, kW; F_3 represents the movable load scheduling cost, yuan; F^{trans} represents the scheduling cost of the transferable load, yuan; n = 1, 2, 3 refer to cooling, heating, and electrical loads, respectively; F_4 represents the environmental cost (only considering the penalty cost of CO_2 emission is considered in this study), yuan; K_c indicates the penalty coefficient for unit carbon dioxide emissions, yuan; η_1, η_2, and η_3 respectively represent the CO_2 MT emission coefficient, GB emission coefficient, and FC emission coefficient of output unit power, *yuan/kg*; and $P_{MT}(t)$, $P_{GB}(t)$, and $P_{FC}(t)$, respectively, represent the output power of MT, output thermal power of GB, and output electric power of FC in period t, kW.

The CO_2 economic punishment model only highlights companies that exceed the carbon quota standard; thus, low-level carbon emissions are not advocated, which will reduce the enthusiasm for production in the park. The carbon trading mechanism considers carbon emissions as a tradable commodity in the market and uses market means to effectively control carbon emissions, which will promote the use of clean energy. The penalty mode of carbon emissions is mainly manifested via the following two aspects: 1) when the actual carbon emission of the enterprise is less than the carbon quota, excess carbon credits can be sold at real-time transaction prices in the market, which is equivalent to reducing the economic cost of the operation of the IES in the park. 2) When the actual carbon emissions of the enterprise are greater than the carbon quota, enterprises are required to purchase excess carbon credits in the market or pay corresponding over-emission fines, which is equivalent to an increase in the operating cost of the IES system in the park. Thus, the introduction of the carbon trading mechanism has changed the composition of the operating costs of the power system, prompting CO_2 sources to incorporate

TABLE 1 | Park IES operating parameters.

Type	Power upper limit/kW	Power lower limit/kW	Operating cost/yuan
Grid power tariff	—	—	Time-of-use
Wind turbine	Forecast	0	0.52
PV	Forecast	0	0.72
GT	200	0	Natural gas price
GB	100	0	Natural gas price

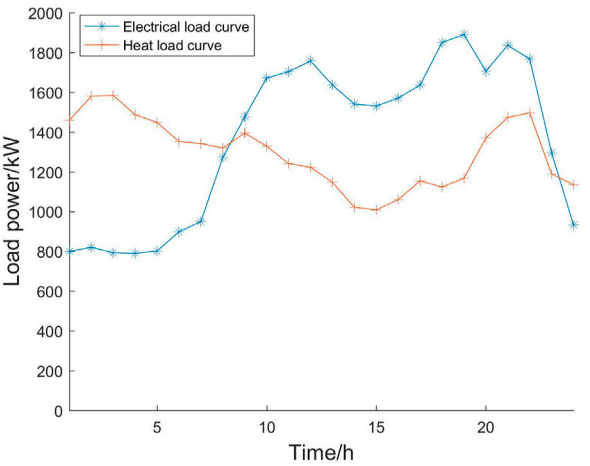

FIGURE 2 | Typical user daily load curve.

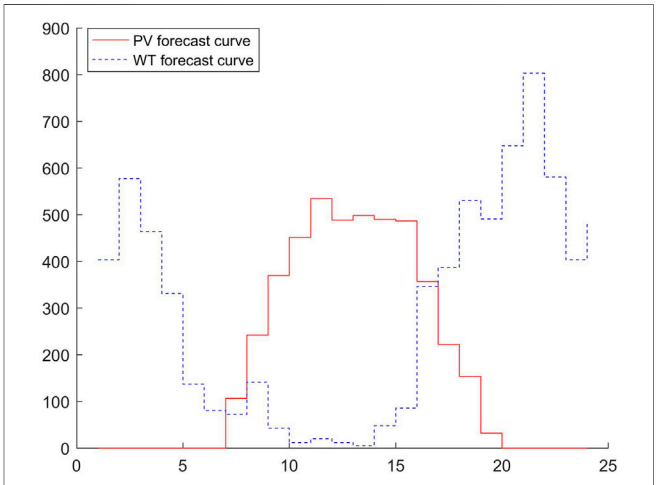

FIGURE 3 | New energy forecast.

carbon emission costs into their optimization goals, formulate optimization strategies based on allocation quotas and market carbon trading prices, and determine carbon emissions from in-house production in the parks. For the aforementioned model, this article uses the CPLEX solver in the YALMIP toolbox to solve the model in the MATLAB environment (Matlab for 2016b).

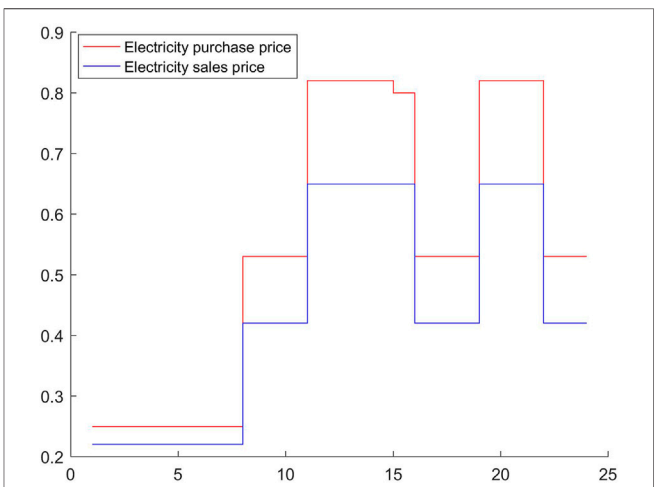

FIGURE 4 | Electricity purchase and sale price by time period.

OPTIMIZATION RESULTS STUDY ANALYSIS

This study considers the IES of a park in northeast China in summer as the research object, and the energy structure diagram of the park is shown in **Figure 1**. These include units such as fans, PV, GT, batteries, and HS tanks, considering factors such as controllable loads and time-of-use electricity prices. The scheduling period is 24 h, and the time period is scheduled in units of 1 h. The operating parameters of the park are shown in **Table 1**.

Basic Data

The output of wind power photovoltaic is not so stable and has strong volatility and randomness. The large-scale wind power photovoltaic is gradually connected to the power grid. At the same time, the power grid requires a real-time balance between power generation and consumption. Generally, the power generation plan will be formulated in advance. The formulation of a power generation plan is generally based on the results of load forecasting and new energy forecasting. Therefore, accurately predicting the output of wind power PV in the future is of great significance for power grid supply and demand balance and economic dispatching. This is why the power grid pays more and more attention to this problem.

The typical daily load curve of the park is shown in **Figure 2**, and the output forecast of WTs and PV units is shown in **Figure 3**.

The energy prices in the optimized scheduling model are time-of-use electricity prices and fixed gas prices. The prices of electricity purchased correspond to the peak, valley, and normal periods, and their price distribution is shown in **Figure 4**. The valley period ranges from early morning 00:00 to 7:00, the purchase price of electricity is 0.25 yuan, and the price of electricity sold is 0.22 yuan. For the peak hours of 10:00–15:00 and 18:00–21:00, the purchased electricity price was 0.82 yuan and the selling electricity price was 0.65 yuan. For the peak period of 21:00–24:00, the electricity purchase price was 0.53 yuan, the electricity selling price was 0.42 yuan, and the price of natural gas was 0.25 yuan/m^3. The proposed energy storage model is a general model under the general energy storage system. Among such general models, the electrical loads on the demand response side mainly include basic loads, translatable electrical loads 1 and 2, transferable electrical loads, and curtailable electrical loads. The thermal loads on the user side mainly include basic thermal loads, translatable thermal loads, and curtailable electrical loads. The heat load of each type of controllable electricity and heat load before optimization are shown in **Figure 5**.

Analysis

To verify the impact of flexible loads on comprehensive energy system management, the following two scenarios were set for comparison. Scenario 1: consider the case of flexible electrical loads that can be shifted, transferred, and participate in system optimization scheduling costs and carbon trading costs. Scenario 2: consider the case without flexible loads and carbon trading. These scenarios presented the same conditions with differing load values. Through optimization scheduling analysis using MATLAB, two optimization results were obtained. **Figure 5** shows the demand response load curve before and after scenario 1 optimization, **Figure 6** presents the output of each energy source, and **Figures 6–8** show the flexible load distribution after optimization.

In **Figure 8**, for the electrical load, during the period 00:00–07:00, the electricity price is in the valley, and the required electricity load is also relatively low. At this time, the electricity price is 0.25 yuan/kWh. WT has no output, and the operating cost of the WT was 0.52 yuan/kWh, which is higher than that of the electricity price; hence, the grid was powered, and the WT provided no output before 8:00. The GT was in the mode of determining electricity by heat; hence, there would be excess electricity to charge the battery. During the period 10:00–15:00 and 18:00–21:00, new energy PV was abundant but similar to the cost of buying electricity from the grid. In such cases, the WT could be effectively utilized as the battery was charged during the period of low electricity prices, such as 00:00–04:00, 15:00–18:00, discharged during periods of high electricity prices such as 10:00–15:00, 19:00–21:00.

For the heat load, most of the heat was provided by the heat recovery system, and the GB and the HS tank were used for supplementary combustion. During the period of 00:00–07:00, the output of the GB reduced the heat output and electrical output of the GT; concurrently, the electrical output of the gas turbine decreased, such that the power dispatch should purchase electricity from the point network, with the excess electricity being stored in the battery, reducing the cost of power dispatching during this period. At 10:00–15:00 and 18:00–21:00, the full power of the GT could also compensate for the shortage of electricity. During the periods of 00:00–01:00, 10:00–11:00, 13:00–15:00, and 18:00–19:00, when the heat load was at a low point, HS can store heat through GB. When the heat load reached its peak, the HS tank released heat and demonstrated peak shaving and valley filling.

Comparing **Figures 8**, **9**, for the flexible electrical load, the translatable load 1 translated from 19:00–22:00 to 05:00–08:00, while the translatable load 2 translated from 11:00–13:00 and 15:00–17:00, and the shiftable loads 1 and 2 were shifted from the high electricity price period to the low electricity price period. Load reduction occurred during the periods of 10:00–15:00 and

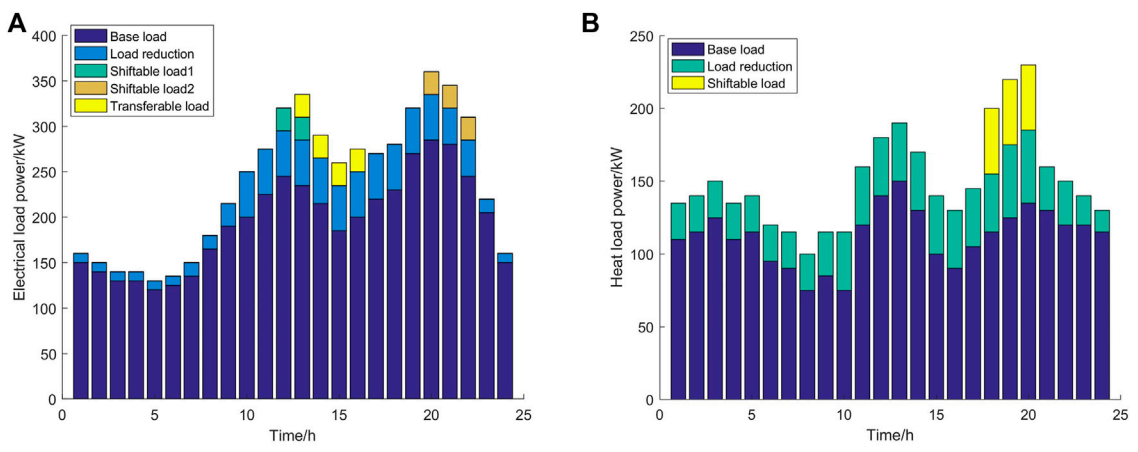

FIGURE 5 | User-side electric and heating load distribution before optimization. **(A)** Electrical load and **(B)** heat load

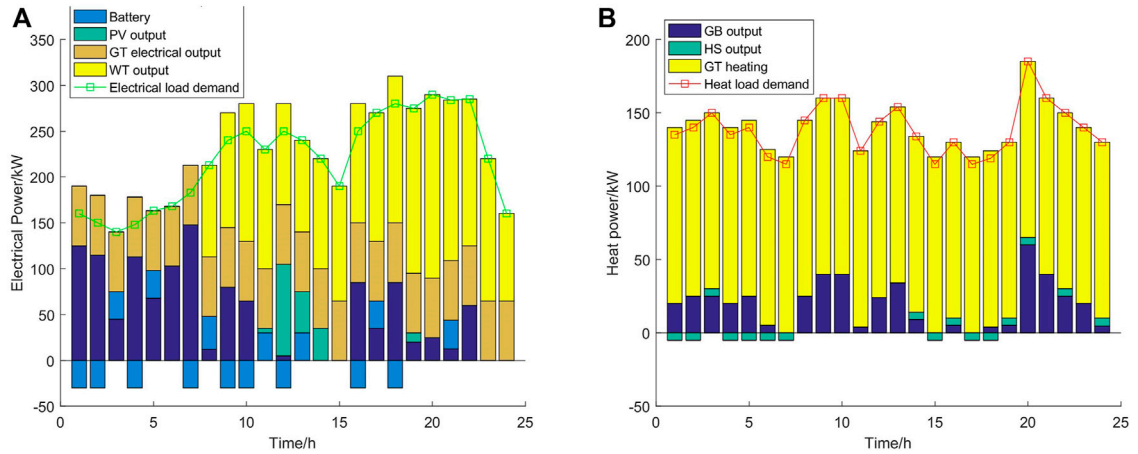

FIGURE 6 | Scenario 1: Balance of electrical load and heat load after optimization. **(A)** Electrical load and **(B)** heat load.

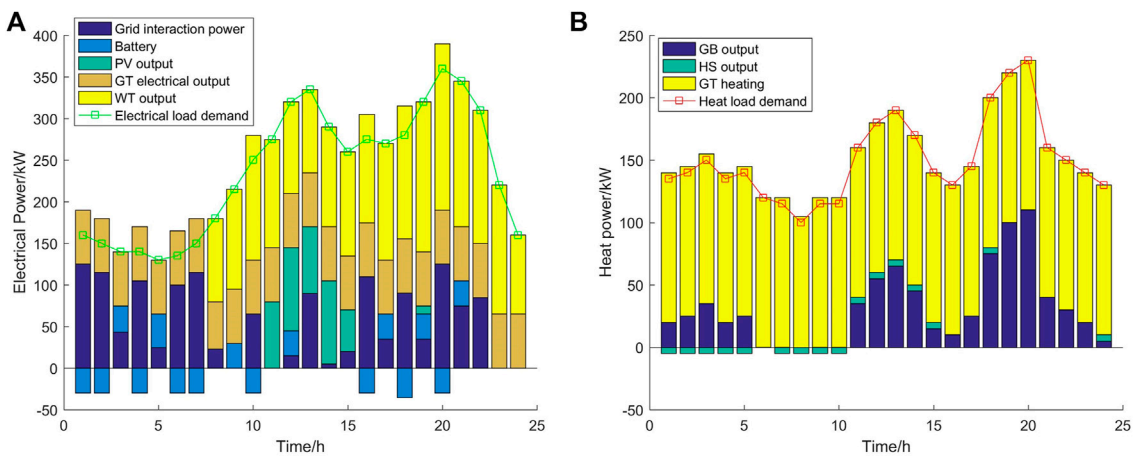

FIGURE 7 | Scenario 2: Balance of electrical load and heat load after optimization. **(A)** Electrical load and **(B)** heat load.

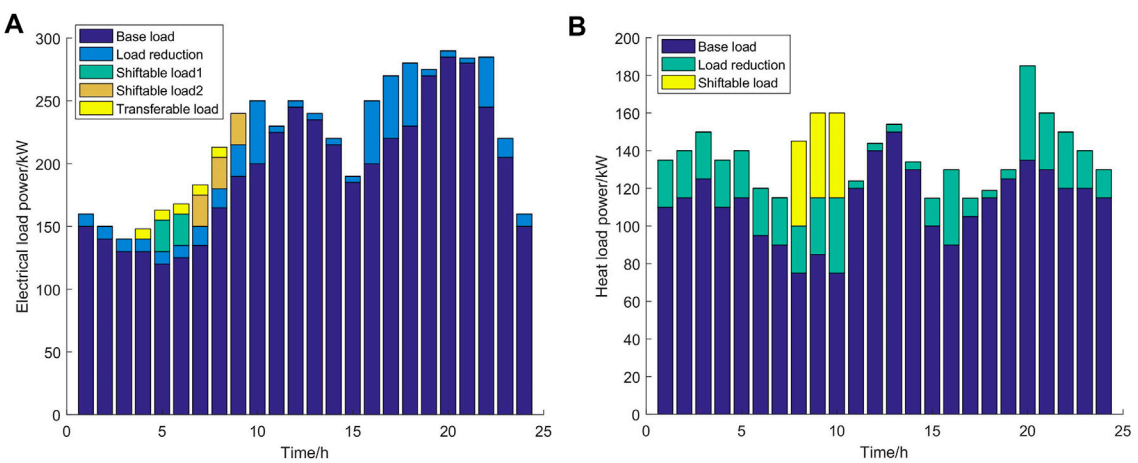

FIGURE 8 | Scenario 1: Distribution of electrical load and heat load after optimization. **(A)** Electrical load and **(B)** heat load.

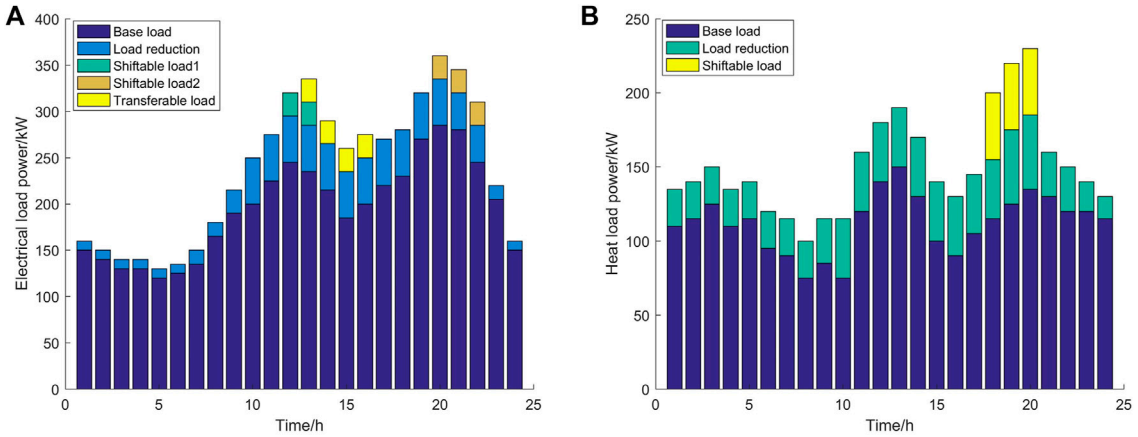

FIGURE 9 | Scenario 2: Distribution of electrical load and heat load after optimization. **(A)** Electrical load and **(B)** heat load.

TABLE 2 | Scheduling results for different scenarios.

Scene	Operating cost (yuan)	Carbon trading cost (yuan)	Total cost (yuan)	New energy output (kwh)	Carbon emission (t)
1	3243	130.58	3373.58	3996.28	2.49
2	3526	—	3526	2898.37	3.12

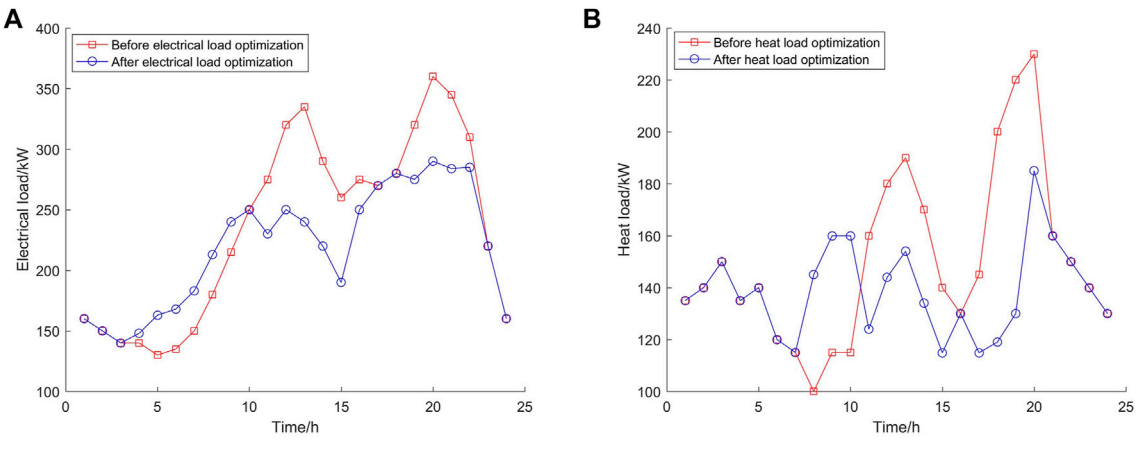

FIGURE 10 | Scenario 1: Electric heating load response curve before and after optimal scheduling. **(A)** Before optimal scheduling and **(B)** after optimal scheduling.

18:00–21:00, mostly during the peak period of electricity prices. For the flexible thermal load, similar to the electrical load, the shiftable load was shifted from the evening peak period to the normal period, which indicated peak shaving, and load reduction further reduced the thermal load. Considering the economic and environmental benefits in the earlier different scenarios, the models of each scenario were solved, and the scheduling results are shown in **Table 2**.

From **Table 2**, scenario 2 did not consider carbon transaction costs. In **Table 2**, the carbon emission cost of scenario 2 was significantly higher than that of scenario 1, and its utilization rate of new energy was only 78.2% of that of scenario 1. The running cost of scenario 2 was approximately 9.1% higher than that of scenario 1. Thus, the orderly control of the controllable power load not only improves the environmental benefits but also optimizes the overall benefits of the IES in the park.

To verify the impact of the introduction of flexible loads and carbon trading on the economic dispatch of the IES in the park, scenarios 1 and 2 were analyzed, and the output of each energy source and the response curve of the electric heat load were obtained, respectively.

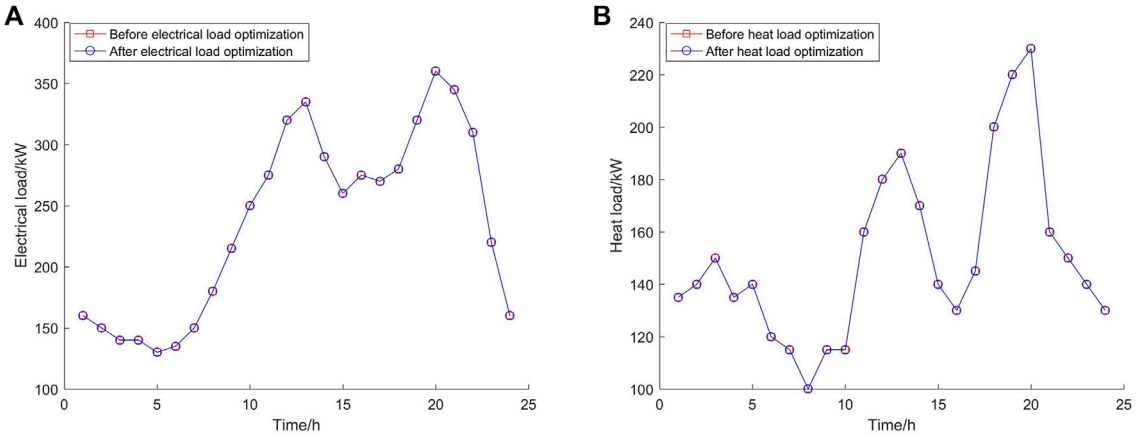

FIGURE 11 | Scenario 2: Electric heating load response curve before and after optimal scheduling. **(A)** Before optimal scheduling and **(B)** after optimal scheduling.

On comparison of **Figures 10** and **11**, it could be concluded that in scenario 1, when the flexible load translation reduction was considered, the overall trend showed that the peak period of electricity and heat consumption shifted like a valley period, with no change in scenario 2. Passing **Figure 10**, we could intuitively conclude that the utilization rate of wind energy and light energy in scenario 1 was higher than that in scenario 2, which is more concentrated in electricity price valleys and normal times. Scenario 1 had a higher utilization rate of clean energy; hence, its electricity purchase cost would be lower than that of scenario 2. The power storage device would shave peaks and fill valleys in different situations. Unlike scenario 2, scenario 1 was favorable for the use of clean energy for energy storage devices.

CONCLUSION

This study proposes an industrial park system model that considers the comprehensive demands of multiple loads of electric and thermal. Through analyzing the structure of the integrated energy system, the characteristics of important components, considering the dispatchable value of multiple loads in integrated energy management, based on the demand response ability and adjustable ability of the electricity and heat loads on the user-side, a mathematical model of the electricity load response on the user-side based on price-based demand is established. To provide a mathematical description of heat load with special properties, a day-ahead scheduling model for the park IES that considers the carbon trading system and controllable load is proposed, and both operating costs and carbon trading costs are considered.

The optimization effect of the carbon trading system on the energy structure of the IES in the park is confirmed by the two settings, and the participation of the controllable load can optimize the comprehensive economic and environmental benefits of the system. Furthermore, the demand response of multiple controllable loads of electric heating exceeds that of a single load. Thus, the following advantages can be obtained by our method: more economic demand response, higher utilization rate of wind energy and solar energy, and fewer users' consumption of energy; based on these advantages, we can extend the suggestion of a carbon trading mechanism into a low-carbon economic strategy which greatly helps for environmental protection and economic operation.

DATA AVAILABILITY STATEMENT

The original contributions presented in the study are included in the article/Supplementary Material; further inquiries can be directed to the corresponding author.

AUTHOR CONTRIBUTIONS

BW: establishes a microgrid model. HS: optimal scheduling strategy. XS: energy storage system.

FUNDING

This work was supported in part by the Scientific and Technological Planning Project of Jilin Province (20190302106GX).

ACKNOWLEDGMENTS

This is a short text to acknowledge the contributions of specific colleagues, institutions, or agencies that aided the efforts of the authors.

REFERENCES

Alipour, M., Zare, K., and Abapour, M. (2018). MINLP Probabilistic Scheduling Model for Demand Response Programs Integrated Energy Hubs. *IEEE Trans. Ind. Inf.* 14, 79–88. doi:10.1109/tii.2017.2730440

Chen, X. Y., Kang, C. Q., O'Malley, M. O., Xia, Q., Bai, J., Liu, C., et al. (2015). Increasing the Flexibility of Combined Heat and Power for Wind Power Integration in China: Modeling and Implications. *IEEE Trans. Power Syst.* 30, 1848–1857. doi:10.1109/TPWRS.2014.2356723

Chen, Y., Gao, Y., and Zeng, B. (2021). "A Hierarchical Optimal Dispatching Method Considering the Flexibility Margin of Regional Power Grid," in 2021 IEEE Sustainable Power and Energy Conference (iSPEC), Nanjing, China, 23-25 Dec. 2021, 589–595.

Dolatabadi, A., and Mohammadi-Ivatloo, B. (2017). Stochastic Risk-Constrained Scheduling of Smart Energy Hub in the Presence of Wind Power and Demand Response. *Appl. Therm. Eng.* 123, 40–49. doi:10.1016/j.applthermaleng.2017.05.069

Hatziargyriou, N., Asano, H., Iravani, R., and Marnay, C. (2007). Microgrids. *IEEE Power and Energy Magazine* 5, 78-94. doi:10.1109/MPAE.2007.376583

Hinton, G. S., Villaseñor, J. L., and Ortiz, E. (2019). The Hintons' Legacy to the Knowledge of the Flora of Mexico. *Bot. Sci.* 97, 447n538. doi:10.17129/botsci.2210

Katiraei, F., Iravani, R., Hatziargyriou, N., and Dimeas, A. (2008). Microgrids Management. *IEEE Power Energy Mag.* 6, 54–65. doi:10.1109/MPE.2008.918702

Li, Z., Wu, W., Wang, J., Zhang, B., and Zheng, T. (2016). Transmission-Constrained Unit Commitment Considering Combined Electricity and District Heating Networks. *IEEE Trans. Sustain. Energy* 7, 480–492. doi:10.1109/tste.2015.2500571

Li, Z., Zhang, F., Liang, J., and Yun, Z. (2015). Optimization on Microgrid with Combined Heat and Power System. *Proc. CSEE* 35, 3569–3576. doi:10.13334/j.0258-8013.pcsee.2015.14.011

Stluka, P., Godbole, D., and Samad, T. (2011). "Energy Management for Buildings and Microgrids," in *Proceedings of the IEEE Conference on Decision and Control* (Orlando, FL, USA: IEEE), 5150–5157. doi:10.1109/cdc.2011.6161051

Vasilj, J., Gros, S., Jakus, D., and Zanon, M. (2019). Day-Ahead Scheduling and Real-Time Economic MPC of CHP Unit in Microgrid with Smart Buildings. *IEEE Trans. Smart Grid* 10, 1992–2001. doi:10.1109/tsg.2017.2785500

Yang, T., Liu, W., Kramer, G. J., and Sun, Q. (2021a). Seasonal Thermal Energy Storage: A Techno-Economic Literature Review. *Renew. Sustain. Energy Rev.* 139, 110732. doi:10.1016/j.rser.2021.110732

Yang, Z., Ghadamyari, M., Khorramdel, H., Alizadeh, S. M. S., Pirouzi, S., and Milani, M. (2021b). Robust Multi-Objective Optimal Design of Islanded Hybrid System with Renewable and Diesel Sources/Stationary and Mobile Energy Storage Systems. *Renew. Sustain. Energy Rev.* 148, 111295. doi:10.1016/j.rser.2021.111295

Conflict of Interest: Author XS was employed by the State Grid Changchun Power Supply Company.

The remaining authors declare that the research was conducted in the absence of any commercial or financial relationships that could be construed as a potential conflict of interest.